Two-Dimensional Spatial Solitary Waves from Traveling-Wave Parametric Amplification of the Quantum Noise

Paolo Di Trapani,[1] Gintaras Valiulis,[2] Walter Chinaglia,[3] and Alessandra Andreoni[1]
[1]*Institute of Mathematical, Physical and Chemical Sciences, University of Milano, Via Lucini 3, 22100 Como, Italy and INFM (Istituto Nazionale di Fisica della Materia), 22100 Como, Italy*
[2]*Department of Quantum Electronics, Vilnius University, 2054 Vilnius, Lithuania*
[3]*2nd Faculty of Sciences, University of Milano, 22100 Como, Italy*
(Received 18 December 1996; revised manuscript received 11 September 1997)

In a single 15-mm lithium triborate crystal, operated at high gain and strong diffraction, we obtained the spatial mode locking of the quantum noise, its amplification up to the pump level, and quasisoliton propagation of the mutually trapped beams. Visible pulses of 1 μJ 1.5 ps were converted, with 50% efficiency, into diffraction-limited superfluorescence, tunable in the range 0.67–2.5 μm. [S0031-9007(97)05012-6]

PACS numbers: 42.65.Tg, 42.50.Lc, 42.65.Yj

The research on the generation and control of 2D transverse structures in traveling-wave (TW) optical systems has been obtaining much attention in recent years, due to its large potential for applications to opto-optical devices: in comparison with the more investigated structures in resonators [1], suitable for optical-memory applications, TW structures offer the unique opportunity of ultrafast (ps-fs) switching and signal addressing, being their speed of response not limited by the dynamic of the feedback mechanism on which resonators are based [2]. Recently, TW filamentation initiated by the quantum noise has been obtained in numerical simulations with a $X^{(3)}$ material [3], and experimentally observed in quantum-noise parametric amplification in a $X^{(2)}$ material [4]. Other structures, like rolls, Bessel beams, vortices, are currently investigated by several research groups. Particularly relevant for the mentioned applications are the structures arising from zero or multiple-order solitonlike propagation, since they can provide robust output profiles controllable in a quasidiscrete manner [2]. In comparison with 2D spatial solitons in saturable-$X^{(3)}$ [5] or in photorefractive [6] materials, those in quadratic media [7] allow faster responses, lower losses, and the possibility of frequency (up or down) conversion. Interesting theoretical investigations were performed on $X^{(2)}$ solitons (or quasisolitons; see, for example, Refs. [8–14]), but experimental demonstration was only reported for second-harmonic generation (SHG) [15].

In this Letter we report the observation of mutual trapping and quasisoliton generation in TW parametric down-conversion from quantum noise amplification. The mechanisms of trapping and soliton generation, which occur in gain saturation in the second portion of the crystal, are similar to those taking place in SHG. Completely different is, on the other hand, the transient process taking place in the first few mm of linear amplification. In fact, while in the case of SHG all the injected fields are intense and coherent laser pulses, in our case both signal and idler are provided by the very weak and incoherent quantum noise. The spatial mode locking of the incoherent signal, occurring with an amplification that exceeds 10 orders of magnitude, together with the broad (>2000 nm) wavelength tunability, are some of the relevant peculiarities of the results that we present.

The experiment, performed at the Optical Non-Linear Processes Laboratory in Como, concerns the characterization of the near and far-field energy-density distribution of the residual pump and of the parametric superfluorescence (the single-pass-amplified quantum noise) generated by 1.5-ps, 0.527-μm pump pulses in a 15-mm lithium triborate (LBO) crystal, operated in type I temperature-tuned noncritical phase matching (i.e., in the absence of transverse walkoff). All of the experimental results, as well as the simulations, refer to signal and idler wavelengths $\lambda_s = 0.83$ μm and $\lambda_i = 1.44$ μm. Results similar to those presented here were obtained across the whole tuning range, 0.67–2.5 μm.

In Fig. 1 we show the measured output-beam parameters versus the input-pump energy E_{p0}, for two input-pump FWHM beam diameters: $\phi_{p0} = 23$ μm, in Fig. 1(a), and $\phi_{p0} = 57$ μm, in Fig. 1(b). In the figure are evident the two regimes of small-signal gain (or linear amplification), in which the pump is not depleted and the (signal + idler) conversion efficiency η increases exponentially with E_{p0}, and that of gain saturation, at greater pump energies. We observed that output pump and signal energies did not increase for E_{p0} exceeding 1 μJ. This can be due either to the fact that a portion of E_{p0} is scattered and not coupled with the detector, or to higher-order nonlinear losses. The large reduction in pump-beam diameter, the matching between output ϕ_p and ϕ_s, the small changes in output profiles in spite of the relevant changes in input-pump energies and diameters, are all phenomena that confirm the existence of mutual trapping and quasisoliton propagation [15].

In Fig. 2 we plot typical single-shot energy-density maps, obtained in regime of gain saturation. The choice

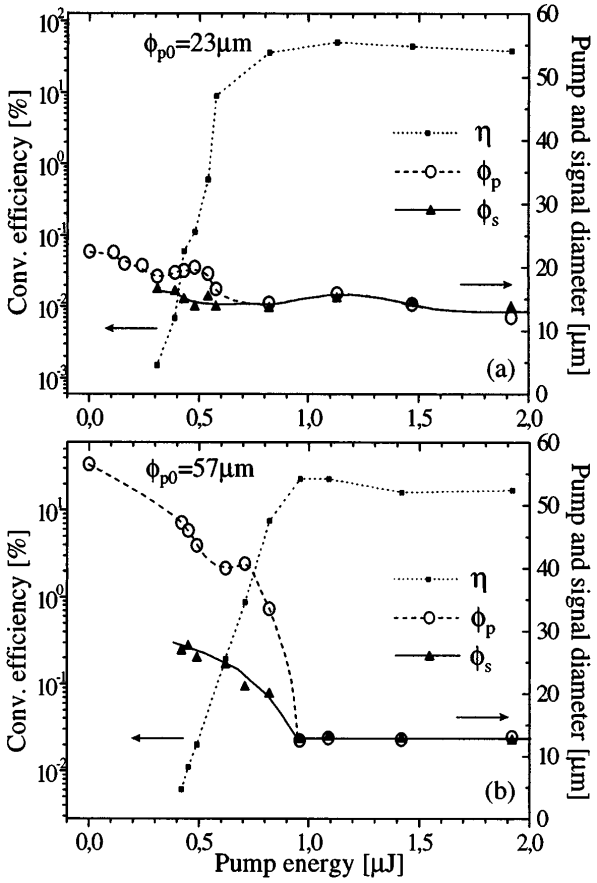

FIG. 1. FWHM diameters of signal ϕ_s and residual pump ϕ_p; conversion efficiency η; lines are guides to the eyes.

of the same scale for the z axis in all maps evidences that similar outputs are obtained in case of two pump beams with similar energies and shape, but different diameters and intensities (the noisy features of the $\phi_{p0} = 57$ μm undepleted pump is due to close-to-threshold operation of the charge-coupled device detector). Note how well the residual-pump and signal beams do match, not only in diameter but also in profile. Pure-$X^{(3)}$ self-focusing was excluded by observing the small effect left upon quenching the parametric interaction by rotating the pump polarization by 90°. From far-field measurements, the divergence of superfluorescence in gain saturation was that of a diffraction-limited Gaussian beam. The space-bandwidth product $\phi_s \Delta\nu_s$ worsened on increasing ϕ_{p0}, as confirmed by the near-field signal-beam profiles in Fig. 3.

In the second part of the experiment we characterized the near- and far-field profiles of the signal superfluorescence obtained in regime of small-signal gain (at low pump intensity), for different pump-beam diameters. Measurements performed with $\phi_{p0} = 23$ μm, $\phi_{p0} = 57$ μm, and $\phi_{p0} = 110$ μm, all with pump intensity $I_{p0} \simeq 10$ GW/cm^2 and $\eta < 0.1\%$, provided clean, almost diffraction-limited superfluorescence beams (e.g., $\phi_s \Delta\nu_s \simeq 0.5$, for $\phi_{p0} = 57$ μm). The beam quality worsened at increasing pump diameter: we measured $\phi_s \Delta\nu_s \simeq 6$ and 25 times the Fourier limit for $\phi_{p0} = 0.4$ and 1.1 mm, respectively, and similar I_{p0} and η values. These results allow us to describe what occurs inside the crystal, at higher pump intensity. This can be done relying upon the $I\phi^4$ scaling law common to all solutions to the three-wave coupled equations [14] in the absence of first-order dispersion. This scaling ensures that, for both $\phi_{p0} = 23$ μm and $\phi_{p0} = 57$ μm, the signal superfluorescence should reach the diffraction limit at the same $\eta < 0.1\%$ value for all the pump intensities covered in Fig. 1. This process of "spatial mode locking" under linear amplification provides the intense and coherent signal beam required for properly seeding the trapping and soliton generation in the last millimeters of saturated interaction. Our simulations (data not shown) indicate that beam profiles such as those in Figs. 2 and 3(b) cannot be obtained within a few mm of gain-saturated interaction if pump depletion is initiated by a structured signal.

We interpret the described transient phenomenon in terms of spatial mode locking of the incoherent quantum noise, relying upon the formal analogy between this process and the temporal mode locking in laser resonators. In mode-locked lasers, transform-limited pulses are generated from the noise level thanks to the combined effect of two competing processes: the reduction in pulse duration, due to the temporal modulation of gain or losses, and the narrowing in (time-domain) spectrum, due to the line shape of the laser amplifier. Analogously, in our parametric converter, diffraction-limited beams are generated from the quantum noise thanks to the competition between the reduction in signal-beam size, due to the transverse gain modulation, and the narrowing in (space-domain) signal spectrum, due to the angular gain profile of the parametric amplifier. The transverse gain modulation, which reduces the signal beam size due to the preferential amplification at the signal-beam center, originates from the transverse profile of the focused pump beam. On the other hand, the angular gain profile is not essentially related with the pump profile, in our regime, as we have verified by numerical simulations: the spatial signal spectrum is not filtered by the gain-induced aperture. Even with infinite (plane-wave) pump, the signal bandwidth decreases during amplification, this spectral narrowing being related to the signal-to-idler phase conjugation in parametric process.

The correctness of our interpretation can be verified in the contest of a simple analytical model, if the pump-beam profile is assumed to not affect the gain angular spectrum and the impact of the spectral narrowing on the evolution of the signal-beam profile is neglected (a correct approximation as long as the two processes do not compete). The FWHM angular gain bandwidth of a parametric amplifier pumped by a plane wave turns out to be

$$\Delta\nu_G = \frac{1}{\pi}\left[\frac{8(\ln 2)\pi^2 n_s^2}{z L_n \lambda_s^2}\right]^{1/4}, \qquad (1)$$

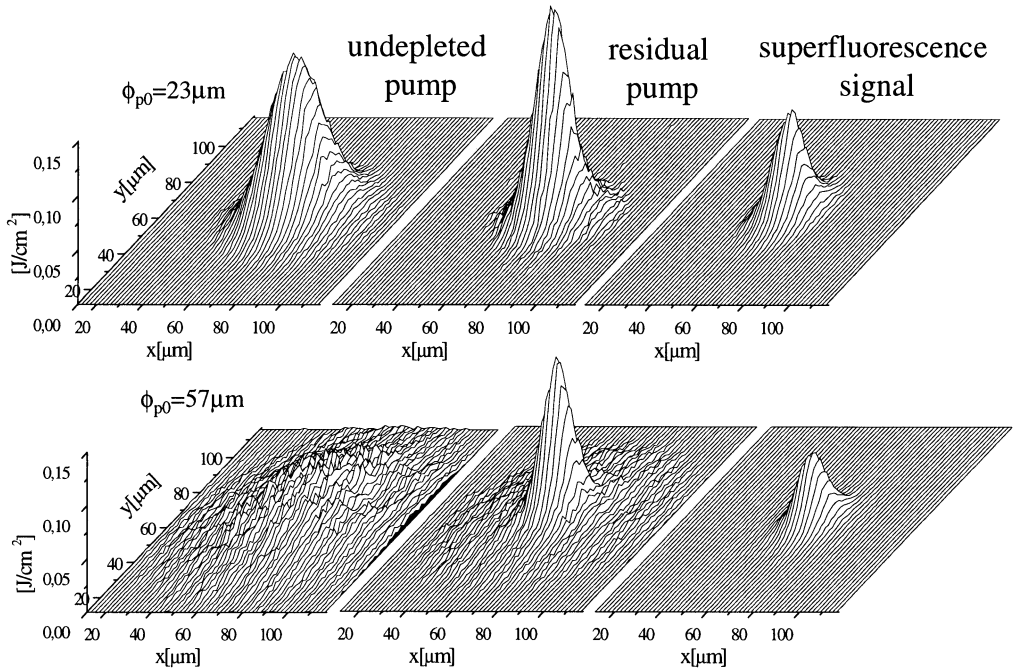

FIG. 2. Single-shot energy-density maps of near-field profiles of signal superfluorescence (right), residual pump (center), undepleted pump (left). Residual and undepleted pump were obtained with the same setup, except for a 1000x ND filter, which was moved from the back to the front of the nonlinear crystal, respectively. Therefore left pictures represent the pump with quenched nonlinear interaction. $\lambda_s = 0.83$ μm. Top: $\phi_{p0} = 23$ μm, $E_{p0} = 0.82$ μm; bottom: $\phi_{p0} = 57$ μm, $E_{p0} = 0.96$ μJ.

where λ_s is the signal wavelength, n_s the refraction index at λ_s, z the propagation coordinate, and L_n the nonlinear length, that is the distance at which the signal intensity is amplified by e times ($L_n[mm] = 1.9/\sqrt{I_p[\mathrm{GW/cm^2}]}$, in our case). Equation (1) holds at degeneracy, in regimes of high amplification and in the absence of transverse walkoff. On the other hand, a signal beam with a profile equal to the gain profile of a (nondiffracting) pump of FWHM diameter ϕ_p would have a diameter

$$\phi_G = \phi_p \sqrt{\frac{2L_n}{z}}\,. \tag{2}$$

In the context of this model we can assume that the two processes strongly compete when $\Delta\nu_G\phi_G$ approaches the Fourier limit. Equations (1) and (2) indicate that this occurs definitely before the onset of gain saturation, in all regimes represented in Fig. 1.

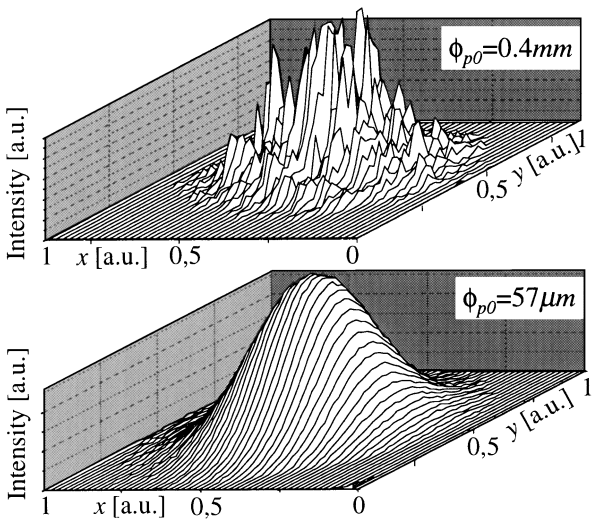

FIG. 3. Near-field energy distribution of parametric superfluorescence in gain-saturation regime. Top: in the absence of trapping ($\phi\Delta\nu = 5.3$); bottom: with trapping ($\phi\Delta\nu = 0.44$).

The dynamic of the spatial mode locking is clarified by our numerical results, which are also in good agreement with the experimental data. Simulations were performed by numerically solving the three-wave coupled equations [14] in the absence of first-order (spatial) dispersion (no lateral walkoff). They account for the coupling between spatial and spectral narrowing, but neglect all time-domain effects, being performed in 2-transverse +1 propagation dimensions (cw approximation). This means that our simulations do not include the temporal gain modulation, the group-velocity mismatch and dispersion, the existence of a fine temporal structure in the signal and in the depleted-pump pulse. Moreover, $X^{(3)}$ contributions are not considered.

In Fig. 4(a) we propose the simulation of the evolution of the pump and signal beam parameters in case of $E_{p0} = 1$ μJ and $\phi_{p0} = 23$ μm.

These results show that three different phenomena dominate in different portions of the crystal: (i) In a first zone (0 mm $< z <$ 6 mm), the incoherent quantum-noise

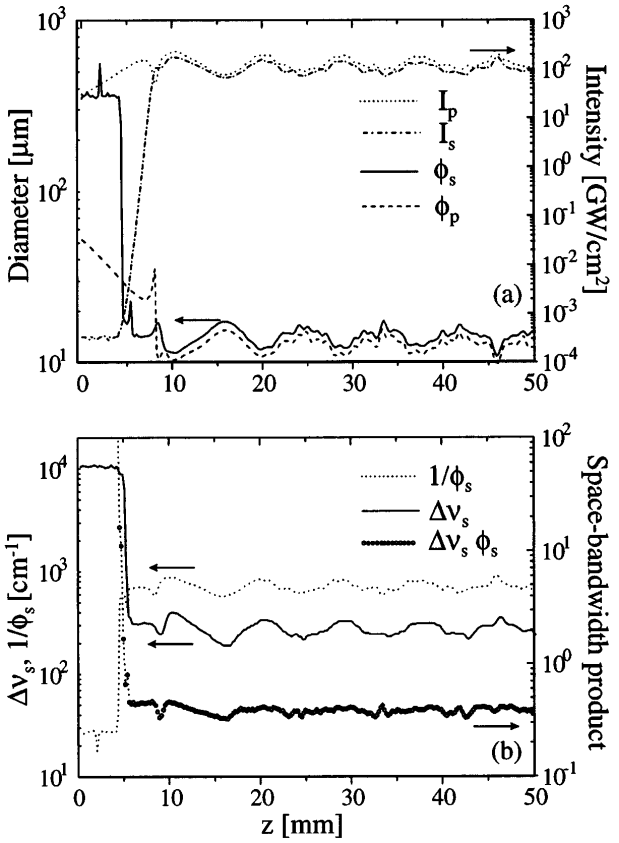

FIG. 4. Numerical simulations of beam-parameters evolution. (a) Pump and signal FWHM diameters ϕ_p and ϕ_s, and intensities I_p and I_s; (b) angular bandwidth $\Delta\nu_s$, space-bandwidth product $\phi_s\Delta\nu_s$, and reciprocal diameter ϕ_s^{-1}, of the signal beam.

signal is mode locked. In the context of our classical and numerical approach, the quantum noise is described by means of a random amplitude-and-phase modulated field, with diameter and bandwidth one order of magnitude larger than those of the pump. Note that ϕ_s and $\Delta\nu_s$ are constant in the first 4 mm, since FWHM values start decreasing only when the mode locking has reduced the noise level below $1/2$ of the peak intensity. In the next 2 mm both ϕ_s and $\Delta\nu_s$ rapidly decrease, until the diffraction limit is obtained at $z = 6$ mm (see the plot of $\phi_s\Delta\nu_s$). (ii) In a second zone (6 mm $< z <$ 8 mm), the mode-locked signal is effectively amplified in condition of small-signal gain (see the exponential growth of I_s), with almost constant ϕ_s and $\Delta\nu_s$. (iii) In a third zone ($z >$ 8 mm), gain saturation, mutual trapping, and quasisoliton propagation occur, with periodical oscillations in intensity, diameter, and bandwidth values, but with almost constant space-bandwidth product. Note that ϕ_s oscillates around 13 μm, in optimum agreement with the experimental value in Fig. 1. Similar results were obtained in the case of $\phi_{p0} = 57$ μm.

In this Letter we have reported on mutual trapping and quasisoliton generation, seeded by weak and incoherent quantum noise. Conditions have been found for which the noise develops into a coherent beam under linear parametric amplification, thus providing the good seed for the trapping and soliton generation process. Work is in progress at our laboratory aimed at demonstrating that the threshold of the process can be lowered to nJ level by using the large-$X^{(2)}$ periodically poled crystals. We believe that this work has great perspectives for several on-field applications in telecommunication networks.

We acknowledge A. Stabinis, A. Piskarskas, and R. Danielius of Vilnius University for helpful discussions. G. V. thanks the Italian National Research Council (C.N.R.) for support.

[1] L. A. Lugiato, Phys. Rep. **219**, 293 (1992).
[2] M. Haelterman, S. Trillo, and P. Ferro, Opt. Lett. **22**, 84 (1997).
[3] E. M. Nagasako, R. W. Boyd, and G. B. Agarwal, Phys. Rev. A **55**, 1412 (1997).
[4] A. Gatti, L. A. Lugiato, G. L. Oppo, R. Martin, P. Di Trapani, and A. Berzanskis, Opt. Expr. **1**, 21 (1997).
[5] V. Tikhonenko, J. Christou, and B. Luther-Daves, J. Opt. Soc. Am. B. **12**, 2046 (1995).
[6] M. Morin, G. Duree, G. Salamo, and M. Segev, Opt. Lett. **20**, 2066 (1995).
[7] Yu. N. Karamzin and A. P. Sukhorukov, JETP Lett. **11**, 339 (1974).
[8] K. Hayata and M. Koshiba, Phys. Rev. Lett. **71**, 3275 (1993).
[9] Qi Guo, Quantum Opt. **5**, 113 (1993).
[10] M. J. Werner and P. D. Drummond, J. Opt. Soc. Am. B **10**, 2390 (1993).
[11] L. Torner, C. R. Menyuk, W. E. Torruellas, and G. I. Stegeman, Opt. Lett. **20**, 13 (1994).
[12] H. T. Tran, Opt. Commun. **118**, 581 (1995).
[13] A. V. Buriak, Y. S. Kivshar, and S. Trillo, Phys. Rev. Lett. **77**, 5210 (1996).
[14] G. I. Stegeman, D. J. Hagan, and L. Torner, Opt. Quantum Electron. **28**, 1691 (1996).
[15] W. E. Torruellas, Z. Wang, D. J. Hagan, E. W. VanStryland, G. I. Stegeman, L. Torner, and C. R. Menyuk, Phys. Rev. Lett. **74**, 5036 (1995).